Tunnelling and Underground Space Technology xxx (xxxx) xxx–xxx

Contents lists available at ScienceDirect

Tunnelling and Underground Space Technology

journal homepage: www.elsevier.com/locate/tust

Repairing a shield tunnel damaged by secondary grouting

Liu Jin-long[a], Omar Hamza[b,*], K. Sian Davies-Vollum[c], Liu Jie-qun[d]

[a] Department of Civil Eng., Hefei University, Hefei 230601, China
[b] Division of Built Environment, University of Derby, Derby DE22 3AW, UK
[c] Environmental Sustainability Research Centre, University of Derby, Derby DE22 1GB, UK
[d] Department of Computer Science and Technology, Hefei University, Hefei 230601, China

ARTICLE INFO

Keywords:
Shield tunnelling
Leakage
Secondary grouting
Track bed
Uplift
Repair
Hefei

ABSTRACT

This paper reports on a repair work which has recently been conducted for a metro tunnel in Hefei city, China. The tunnel has been originally constructed using shield method where synchronous grouting was used to fill the gaps between the tunnel segments and soil. Following a regular maintenance inspection of the tunnel, several leakage issues were identified between three stations. Secondary grouting was adopted as a solution to block the tunnel leakage, however, shortly after the start of grouting work, the track and track bed were found to be unevenly uplifted with significant cracks in the tunnel's segments. The paper describes and discusses key aspects of this case study including ground conditions, leakages patterns of the tunnel, recorded volumes and injection pressure of the secondary grouting, as well as survey data of track displacement and segment cracks. The investigation confirmed that the situation was caused by an inappropriate implementation of the secondary grouting, particularly by high grouting pressure (significantly higher than the geostatic pressure), large volumes of injected grout, and poor selection of grouting locations. Ground Penetrating Radar (GPR) was conducted to inspect the tunnel conditions before commencing the structural repair work, which revealed that there were no voids under the track bed of the affected zone. The study presents simplified strategies used to repair the damage while maintaining minimum disturbance to the affected segments.

1. Introduction

As a safe, fast, efficient and environmentally friendly form of transportation, underground trains (metro) have quickly become the first choice for many large cities around the world to solve their traffic congestion. In China, more than 40 cities have either carried out or are planning to construct metro tunnels. The length of urban metros is expected to reach 6000 km by 2020 (He et al., 2015), covering the major cities of China.

Over the past decades, the tunnelling industry has developed a series of construction methods addressing various geological, hydrological, technical, and economic challenges. These methods have been developed from the traditional single open-cut and cut-and-cover to more advanced techniques such as the shield method (Guo and Wan, 2004). The shield method has been widely used in urban areas because it has little disturbance to the surrounding environment, ensures rapid construction and is better adapted to water-rich soft stratum. In the process of shield tunnelling, concrete segments are gradually assembled while leaving the shield tail. However, as the shield shell inner diameter is greater than the outer diameter of the segment lining, gaps inevitably emerge between the segments and soil. If these gaps are not filled in time, stress release occurs in the soil around the segments leading to ground surface subsidence. For any tunnelling technique, it is essential to avoid ground subsidence and water leakage during and after construction. In shield tunnels, these risks are managed by grouting (Tang et al., 2016).

Grouting is generally subdivided into different types depending on its function, implementation time and location. If cement slurry is injected from a grouting pipe at the shield tail to the outer wall of the segment, it is called "grouting at shield tail" (Ye, 2007). Alternatively, cement slurry might be injected from grouting holes within segments, into the outer wall after the shield has advanced some distance; this is known as "grouting through segments" (Ye, 2007). The two types of grouting, explained above, are synchronous with shield tunnelling thus are categorised as "synchronous grouting". Synchronous grouting fills the gaps between soil and segment, which can help to alleviate soil stratum deformation, ensure uniform stress of the lining, improve the impermeability of shield tunnel lining, fix the position of the segment lining, and transfer the loads of the tunnel and the other auxiliary facilities to the foundation soil (Ye et al., 2015).

* Corresponding author.
E-mail address: o.hamza@derby.ac.uk (O. Hamza).

https://doi.org/10.1016/j.tust.2018.07.016
Received 2 February 2018; Received in revised form 27 June 2018; Accepted 8 July 2018

According to the Chinse technical code (Ministry of Construction of the PRC, 1999), the volume of synchronous grouting should be 130–180% of the volume of gap generated between soil and segments during shield tunnelling. However, in reality, ground subsidence can not be restrained completely even if synchronous grouting volume reached 180% of the gap size. This is because synchronous grouting slurry cannot completely, fill the gap between the segments and soil and some of the slurries are infiltrated and lost if the soil has a large coefficient of permeability. In addition, synchronous grouting experiences 1.4% volume shrinkage during solidification (Zheng, 2015). Therefore, a gap or void would still exist between segments and soil after synchronous grouting work. As a consequence, water seepage may occur in the tunnel through the voids and crack zone, or further settlement of ground may take place due to the existence of voids (Wu et al., 2013; Chi, 2015; Li et al., 2016). Thus, there is a need to fill the remaining voids by further grouting. Such grouting is carried out after the completion of construction and is known as “secondary grouting”.

Previous research conducted on grouting of shield tunnels (Komiya et al., 2001; Kasper and Meschke, 2006a; Stille and Gustafson, 2010; Butrón et al., 2010; Yong and Breitenbücher, 2014) has established that the selection and control of grouting pressure are key for effective and successful implementation of almost all grouting types. If the grouting pressure is significantly large in comparison with in-situ ground stresses, segments can be uplifted, dislocated, cracked, crushed or destroyed, and grouting slurry might flow inside the tunnel. If the grouting pressure is too small, a gap or void may remain unfilled and thus ground surface subsidence can occur. Therefore, grouting pressure must be chosen properly during shield tunnelling (Li et al., 2006; Gou, 2013; Kasper and Meschke, 2006b).

This paper reports on the unsuccessful application of secondary grouting which was used in a shield tunnel in Hefei city, capital of Anhui province in China in December 2015. The secondary grouting was selected to treat leakage issues. However, the grouting work led to track, and track bed uplift with several cracks appearing on tunnel segments. The paper describes and discusses key aspects of this case study including ground conditions, leakages patterns of the tunnel, records of injection pressure and volume of the secondary grouting, as well as survey data of track displacement and segment cracks. The investigation revealed that injection pressure and volume of the grouting were too high and applied asymmetrically, which induced uneven uplift of the track and track bed as well as significant cracks in the tunnel segments. Ground Penetrating Radar (GPR) was conducted to inspect the tunnel conditions to inform the repair work. The study presents a simplified approach to repair the structural damage and leakage, with minimum disturbance to the affected segments. The outcome of this work can be used as a case study by the tunnel engineers who are involved with similar maintenance work for shield tunnels.

2. General description of the tunnel construction

Metro line 1 of Hefei city is a key route connecting the north and south of the city, with a total length of 29.06 km and 26 stations. Part of this line, the focus of this study, extends over three stations: Yungu road station, Nanning road station and Guiyang road station. The line between these stations consists of two parallel circular tunnels with a spacing of 15.0 m, as shown in Fig. 1, and was built using the shield construction method.

This tunnel was excavated by a ZTE6250 Earth Pressure Balance (EPB) shield machine, with a diameter of cutter head of 6280 mm, an opening rate of cutter head about 45%, and a driving torque 5700 kN·m. The whole length and weight of the EPB shield machine are about 85 m and 450 tonnes respectively. The maximum total thrust of the propulsion system is 42,575 kN, and the cylinder stroke is 2100 mm. The speed of shield tunnelling is kept as constant as possible at about 15–20 mm/min. The shield lining is stagger-jointed assembled with six blocks of C50 reinforced concrete segments, including three standard blocks, two adjacent blocks and a seal roof block in each ring. The segment has an inner diameter of 5400 mm, outer diameter 6000 mm, thickness 300 mm and width of 1.50 m. Segments are connected with each other by bolts, using 16 ring joint bolts of M27 (i.e. 27 mm diameter) and 12 longitudinal connecting bolts (M27) in each ring. The tunnel section is shown in Fig. 2, and a photograph of the tunnel is shown in Fig. 3.

In order to ensure quality implementation of synchronous grouting during the shield tunnelling, the contractor carried out standard testing on the slurry used for the grouting work. The testing included slurry composition, mixture proportion, slurry mixing process, and slurry properties. The slurry components and mixture proportion of the synchronous grouting are presented in Table 1, as extracted from as-built documents of the tunnel. During the slurry mixing, the following are recorded: mixture ratio, slurry consistency and slurry volume used for each ring of the segments.

3. Geological and geotechnical conditions

The existing geological information indicates there is an engineering fill at the ground surface, underlain by Quaternary sediments and Cretaceous sandy mudstone extending to the maximum depth of investigation (40 m below ground surface). The working face of the shield is mainly located in a clay layer within the Quaternary sediments; the clay is coded as “3” (Fig. 4). This clay is described as pale yellow or brown, hard plastic, medium compressibility, smooth and glossy cut surface, high dry strength containing iron-manganese concretions, It has a bearing capacity of 240 kPa according to the engineering geological survey report. The physical and mechanical parameters for each soil layer (extracted from the report) are summarised in Table 2, where γ is the unit weight of soil (kN/m^3), E_{s1-2} is the compression modulus (MPa), C_u is the undrained cohesion (kPa), K_0 is the lateral pressure coefficient of soil at rest, k_v and k_h are the vertical and horizontal coefficient of permeability (m/s), respectively.

Expansive soil is one of the characteristics of ground conditions in Hefei city. This type of soil exhibits a significant volume change (shrinking and swelling) when subjected to change in water content. In the proximity of tunnels, this volumetric change can produce excessive stresses on underground structures leading to cracks. In the process of shield tunnelling, the excavated soil is expected to lose some of its water content at locations exposed to the construction working face, while water content increases in the soil located behind the tunnel segments due to water dissipated from grouting material. An expansive soil would shrink and repeatedly swell during shield tunnelling, which impacts shield segments (Li, 2014). Therefore, it is necessary to determine the relevant engineering properties of such soils to assess the effect of swell-shrink behaviour on the tunnel. The expansiveness indices of each soil layer are presented in Table 3, whereδ_{ef} is the free swelling ratio (%), δ_{e50} is the swelling ratio (%), λ_s is coefficient of shrinkage, P_e is the swelling force (kPa).

During the ground investigation, perched groundwater was detected within the first layer, with a maximum depth of 5.3 m below ground surface. The perched water is mainly recharged by atmospheric precipitation and paddy field irrigation and discharged by evaporation at the surface. Although this groundwater is located above the shield working face, it is believed to have no direct influence on the shield tunnelling construction. This is because the coefficient of permeability of the ground is very small (see Table 2), which can prevent any significant water seepage into the working face within the short time-scale of the construction. However, after the completion of tunnel construction, long-term seepage might continue toward voids around the tunnel, increasing the water pressure with time and thus causing the reported leakage problem. The existence of voids was confirmed by the pre-repair inspection work carried out for the tunnel as presented in Section 7.

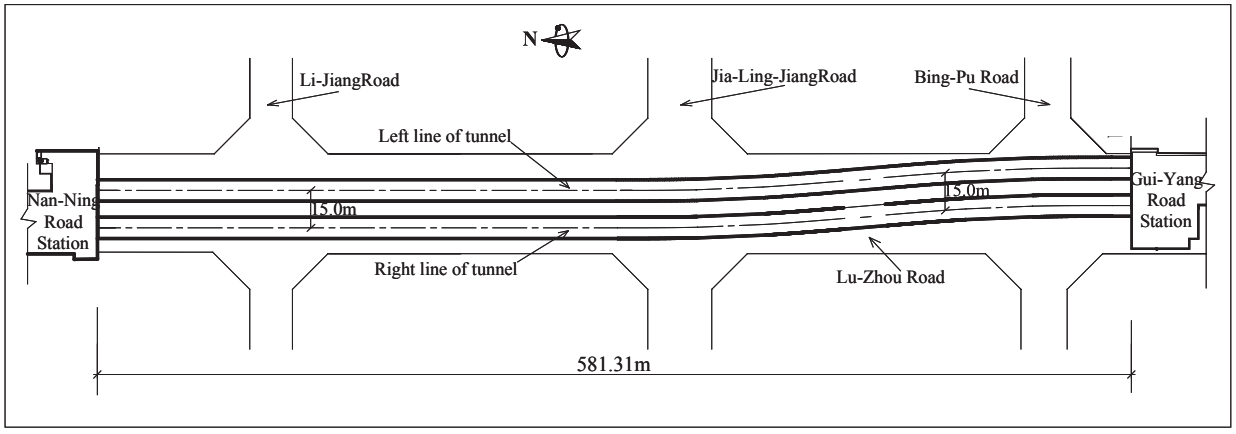

Fig. 1. Typical layout of metro line 1 in Hefei city: from Nanning road station to Guiyang road station.

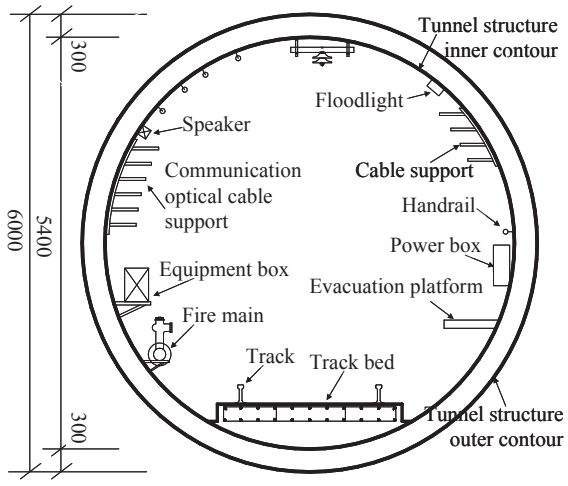

Fig. 2. Tunnel section diagram.

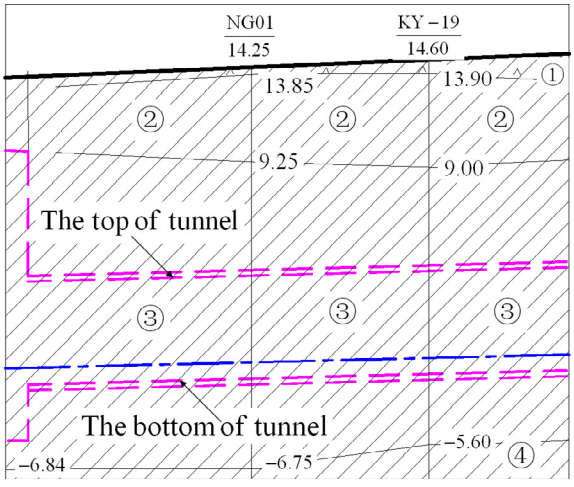

Fig. 4. Typical geological profile of metro line 1 in Hefei city.

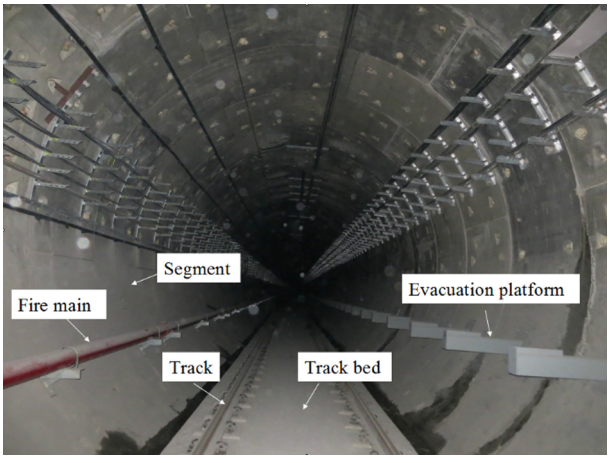

Fig. 3. Photo showing the actual tunnel.

Table 1
Composition of the synchronous grouting slurry.

Volume	Fly ash (kg)	Cement (kg)	Sand (kg)	Bentonite clay (kg)	Water (kg)
1.0 m^3	385.0	200.0	310.0	50.0	270.0

Table 2
Physical and mechanical properties of each soil layer.

Stratum code	Type	γ (kN/m^3)	E_{s1-2} (MPa)	C_u (kPa)	K_0	k_v (m/s)	k_h (m/s)
②	Clay	19.9	11.0	47.0	0.47	6.9e−9	6.9e−9
③	Clay	20.0	12.0	50.0	0.45	2.3e−9	3.47e−9
④	Clay	20.0	14.0	52.0	0.43	2.3e−9	3.47e−9

Table 3
Expansiveness indices of each soil layer.

Stratum code	Type	δ_{ef} (%)	δ_{e50} (%)	λ_s	P_e (kPa)
②	Expansive soil	59.0	0.60	0.43	60.0
③	Expansive soil	59.0	0.54	0.45	60.0
④	Expansive soil	56.0	1.35	0.57	70.0

4. Leakage in the tunnel

The waterproofing standard for this project was designed as grade II, according to the relevant national codes in China (Ministry of Construction of the PRC, 2008). For this grade, the drip-leak of water is not allowed on the roof of the tunnel, but a small amount of water staining is acceptable on tunnel walls. Specifically, the total stained area should not be larger than 2‰ of the total waterproof area, with no more than three wet stains at any 100 m^2 waterproof area, and a maximum area of a single wet stain not larger than 0.2 m^2.

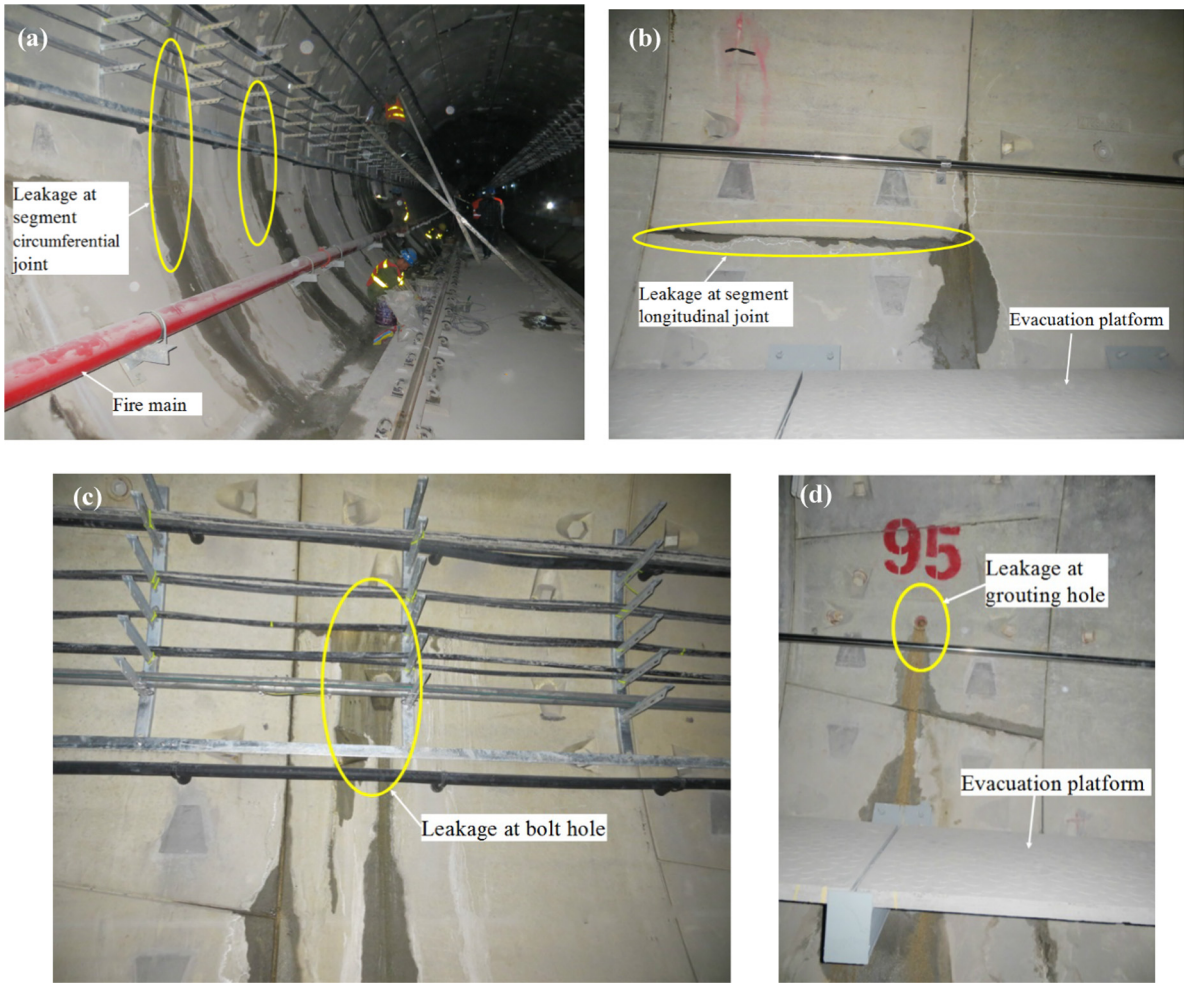

Fig. 5. Typical leakages found in the tunnel: (a) Leakage at circumferential joints of segments, (b) Leakage at a longitudinal joint of segments, (c) Leakage at a bolt hole, (d) Leakage at a grouting hole.

Furthermore, the average seepage quantity of each water leakage should not exceed 0.05 L/(m^2·d), and the total seepage quantity of water leakage at any 100 m^2 waterproof area should not be more than 0.15 L/(m^2·d).

Although it has been reported that the contractor carried out the works according to best practice, there were obvious leakages at segments' joints and bolt holes (Fig. 5), which do not meet the design requirements mentioned above. The initial assessment indicated that perched groundwater had leaked through weak points created by several factors, including (i) dislocation between segments, which reduces the effective area of rubber seal between segments; (ii) fragmentation of segments caused by collision during transporting or assembling, resulting in poor installation of waterstop; (iii) sediment or slurry trapped between segment and waterstop, (iv) bolts between segments not installed tightly, (v) loose plugging of the grouting hole.

5. Leakage treatment with secondary grouting causing damage in the tunnel

The number of wet stains and the average seepage locations in the tunnel did not meet the serviceability requirements, so there was a need to carry out leakage treatment for the tunnel. As part of this maintenance work, an initial study was carried out in order to ensure that the optimum design was developed and to inform decision making. The secondary grouting method, which is commonly used for shield tunnels, was selected to remediate the leakage. A cement-sodium silicate binary slurry was applied to the grouting using the following properties: (i) a weight ratio of water and sodium silicate in sodium silicate slurry of 3:1, (ii) a weight ratio of water and cement in cement slurry of 1:1, (iii) and a volume mixing ratio of cement slurry and sodium silicate slurry of 1:1. Along the tunnel, grouting injection was carried out at grouting holes of the nearest segment to the leakage point with grouting holes located in the middle of segments.

In addition to the selection of injection location, the range of pressure played a key factor in the successful application of secondary grouting. If grouting pressure is too small, slurry may not reach the leakage point, particularly when the tunnel is surrounded by high groundwater pressure. However, if grouting pressure is too large, there is an increased risk of cracking the tunnel segment lining. Therefore, injection pressure control is of great significance to the safety of

Table 4
Typical volume of secondary grouting used in the project.

Chainage (k25+)(m)	424.765	426.265	427.765	430.765	435.265	438.265	439.765	448.765	454.765	456.265	457.765	460.765	463.765	466.765
Volume(m^3)	5.0	8.0	8.0	8.0	8.0	8.0	8.0	8.0	8.0	8.0	8.0	8.0	8.0	8.0

Table 5
Survey data of the left-line of the tunnel at K25 + 412 to K25 + 488.

No.	Chainage (m)	Measured east coordinate of mid line (m)	Measured north coordinate of mid line (m)	Measured track surface elevation (m)	Designed track surface elevation (m)	Deviation of track surface (m)	Deviation of left elevation (m)	Deviation of right elevation (m)	Measured super-elevation (m)	Designed super-elevation (m)	Deviation of super-elevation (m)
1	k 25 + 412.96	28052.498	9937.773	4.533	4.525	0.002	0.007	0.008	−0.001	0.000	−0.001
2	k 25 + 415.965	28052.498	9934.768	4.528	4.519	0.002	0.007	0.010	−0.003	0.000	−0.003
3	k 25 + 418.970	28052.498	9931.763	4.522	4.513	0.002	0.008	0.009	−0.001	0.000	−0.001
4	k 25 + 421.886	28052.499	9928.847	4.516	4.507	0.001	0.007	0.009	−0.002	0.000	−0.002
5	k 25 + 424.765	28052.501	9925.968	4.513	4.501	−0.001	0.011	0.012	−0.001	0.000	−0.001
6	k 25 + 428.822	28052.505	9921.911	4.522	4.493	−0.005	0.029	0.029	0.000	0.000	0.000
7	k 25 + 431.789	28052.504	9918.945	4.537	4.487	−0.004	0.050	0.049	0.001	0.000	0.001
8	k 25 + 434.795	28052.504	9915.938	4.545	4.481	−0.004	0.065	0.062	0.003	0.000	0.003
9	k 25 + 437.768	28052.504	9912.965	4.546	4.473	−0.004	0.075	0.073	0.002	0.000	0.002
10	k 25 + 440.757	28052.505	9909.977	4.539	4.463	−0.005	0.077	0.076	0.001	0.000	0.001
11	k 25 + 443.712	28052.504	9907.021	4.526	4.451	−0.004	0.075	0.074	0.001	0.000	0.001
12	k 25 + 446.722	28052.506	9904.012	4.509	4.437	−0.006	0.073	0.071	0.002	0.000	0.002
13	k 25 + 449.645	28052.503	9901.088	4.492	4.422	−0.003	0.070	0.069	0.001	0.000	0.001
14	k 25 + 452.698	28052.502	9898.036	4.466	4.405	−0.002	0.061	0.061	−0.001	0.000	−0.001
15	k 25 + 455.680	28052.501	9895.053	4.433	4.386	−0.001	0.048	0.047	0.001	0.000	0.001
16	k 25 + 458.656	28052.499	9892.077	4.403	4.365	0.001	0.038	0.038	0.000	0.000	0.000
17	k 25 + 461.618	28052.499	9889.115	4.373	4.343	0.001	0.029	0.031	−0.002	0.000	−0.002
18	k 25 + 464.574	28052.500	9886.159	4.342	4.319	0.000	0.022	0.024	−0.002	0.000	−0.002
19	k 25 + 467.593	28052.500	9883.140	4.310	4.293	0.000	0.018	0.018	0.000	0.000	0.000
20	k 25 + 470.538	28052.501	9880.195	4.279	4.265	−0.001	0.014	0.014	−0.001	0.000	−0.001
21	k 25 + 473.472	28052.500	9877.261	4.247	4.236	0.000	0.010	0.011	−0.001	0.000	−0.001
22	k 25 + 476.451	28052.500	9874.283	4.212	4.205	0.000	0.007	0.007	0.000	0.000	0.000
23	k 25 + 479.438	28052.500	9871.295	4.175	4.172	0.000	0.003	0.003	0.000	0.000	0.000
24	k 25 + 482.396	28052.501	9868.337	4.140	4.137	−0.001	0.003	0.003	0.000	0.000	0.000
25	k 25 + 485.428	28052.501	9865.306	4.105	4.100	−0.001	0.005	0.005	0.000	0.000	0.000
26	k 25 + 488.332	28052.500	9862.401	4.066	4.063	0.000	0.003	0.004	0.000	0.000	0.000

segment structure during secondary grouting. The grouting pressure in this project was set by the contractor at approximately 0.4 MPa. Typical volumes of injected grout recorded at some positions are shown in Table 4.

Surveying showed that a week after the start of the secondary grouting, the left and right elevation of the track, as well as the elevation of track surface had been differently uplifted. The survey data of the lift-line of the track are presented in Table 5 and 6, where the "midline" is the symmetrical centre line of the two parallel tracks, "east coordinate" is the coordinate of east-west direction, "north coordinate" is the coordinate of south-north direction, "left elevation" is the elevation of left track, and "right elevation" is the elevation of right track, "change of elevation" means the difference between designed value and measured value.

The change of track's elevation at two positions is shown in Fig. 6. There is obviously uplift of the track following the implementation of the secondary grouting, with a maximum value of 7.7 cm. The uplift elevation is different at different positions of the track, for examples at

Table 6
Survey data of the left-line of the tunnel at K25 + 671 to K25 + 749.

No.	Chainage (m)	Measured east coordinate of mid line (m)	Measured north coordinate of mid line (m)	Measured track surface elevation (m)	Designed track surface elevation (m)	Deviation of track surface (m)	Deviation of left elevation (m)	Deviation of right elevation (m)	Measured super-elevation (m)	Designed super-elevation (m)	Deviation of super-elevation (m)
1	k 25 + 671.136	28052.503	9679.648	−0.149	−0.157	−0.003	0.008	0.008	0.001	0.000	−0.001
2	k 25 + 674.725	28052.504	9676.059	−0.239	−0.247	−0.004	0.008	0.007	0.001	0.000	−0.001
3	k 25 + 680.684	28052.503	9670.100	−0.383	−0.392	−0.003	0.009	0.008	0.001	0.000	−0.001
4	k 25 + 685.441	28052.503	9665.344	−0.491	−0.499	−0.003	0.007	0.008	0.000	0.000	0.000
5	k 25 + 690.165	28052.503	9660.619	−0.589	−0.597	−0.003	0.009	0.008	0.001	0.000	−0.001
6	k 25 + 694.959	28052.503	9655.825	−0.682	−0.690	−0.003	0.008	0.008	0.000	0.000	0.000
7	k 25 + 699.687	28052.501	9651.097	−0.767	−0.774	−0.001	0.006	0.007	−0.001	0.000	0.001
8	k 25 + 704.473	28052.505	9646.311	−0.842	−0.851	−0.005	0.008	0.010	−0.002	0.000	0.002
9	k 25 + 709.192	28052.505	9641.592	−0.904	−0.920	−0.005	0.015	0.017	−0.002	0.000	0.002
10	k 25 + 712.159	28052.505	9638.625	−0.936	−0.959	−0.005	0.022	0.024	−0.003	0.000	0.003
11	k 25 + 715.756	28052.504	9635.028	−0.968	−1.003	−0.004	0.034	0.035	−0.002	0.000	0.002
12	k 25 + 718.707	28052.503	9632.077	−0.992	−1.036	−0.003	0.045	0.043	0.001	0.000	−0.001
13	k 25 + 721.724	28052.501	9629.060	−1.014	−1.066	−0.001	0.053	0.052	0.001	0.000	−0.001
14	k 25 + 724.642	28052.499	9626.142	−1.036	−1.093	0.001	0.057	0.057	0.000	0.000	0.000
15	k 25 + 727.631	28052.497	9623.154	−1.057	−1.117	0.003	0.060	0.060	0.000	0.000	0.000
16	k 25 + 730.607	28052.499	9620.177	−1.091	−1.138	0.001	0.047	0.047	−0.001	0.000	0.001
17	k 25 + 733.625	28052.499	9617.159	−1.124	−1.157	0.001	0.033	0.032	0.001	0.000	−0.001
18	k 25 + 736.72	28052.500	9614.064	−1.159	−1.172	0.000	0.014	0.012	0.002	0.000	−0.002
19	k 25 + 736.697	28052.500	9614.087	−1.164	−1.172	0.000	0.009	0.008	0.001	0.000	−0.001
20	k 25 + 739.96	28052.504	9610.825	−1.190	−1.185	−0.004	−0.004	−0.005	0.001	0.000	−0.001
21	k 25 + 743.183	28052.502	9607.601	−1.200	−1.195	−0.002	−0.005	−0.005	−0.001	0.000	0.001
22	k 25 + 746.146	28052.501	9604.638	−1.207	−1.201	−0.001	−0.006	−0.006	0.000	0.000	0.000
23	k 25 + 749.105	28052.501	9601.679	−1.212	−1.207	−0.001	−0.005	−0.005	0.000	0.000	0.000

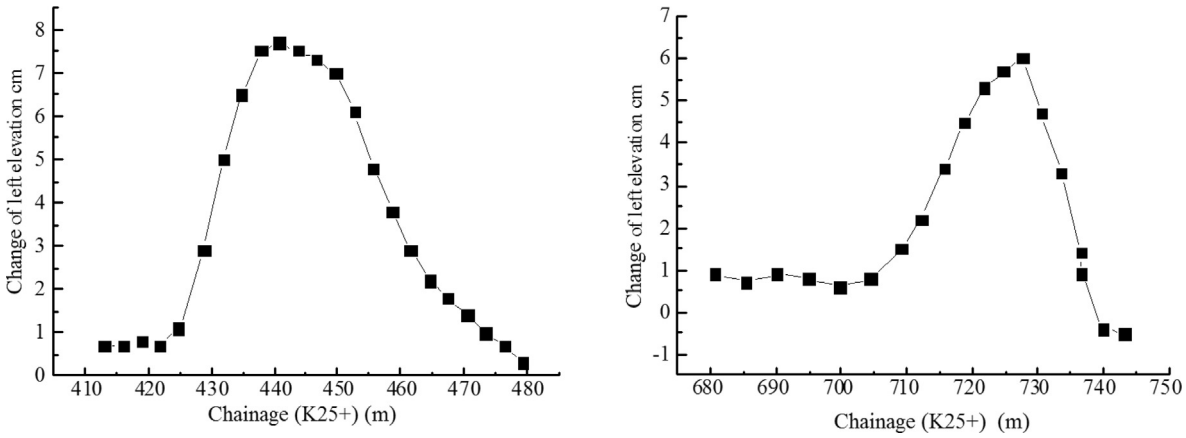

Fig. 6. Typical elevation change of track.

the position K25 + 440 m (i.e. distance to reference point is 25 km and 440 m) and K25 + 725 m the elevation uplift reaches its local peak value, but the corresponding value adjacent to these positions is small (about 1.3 cm). This indicates that differential uplift of segments happened during the secondary grouting.

The differential uplift with the segments produced different modes of structural problem, such as cracks, fragments and dislocation, as shown in Fig. 7.

6. Discussion on the tunnel damage

The cause of track uplift was initially analysed based on the secondary grouting parameters and the field survey data. The analysis indicated the following:

(i) The uplift of track occurred at positions of secondary grouting, while there is no significant change in the segments without secondary grouting. Therefore, it can be inferred that the track uplift is caused by the secondary grouting.
(ii) The value of grouting (injection) pressure of secondary grouting (0.4 MPa) complies with relevant Chinese codes GB50299-1999 and GB50108-2008 (Ministry of Construction of the PRC, 1999 and 2008). However, this value is almost equivalent to typical geostatic pressure (vertical total stress) at 20 m below ground surface. With a buried depth of only 7.8–10.2 m for the tunnel's roof and 13.8–16.2 m for the tunnel's base, the geostatic pressure around

Fig. 7. Typical structural problems observed within the tunnel' segments following the application of secondary grouting: (a) Crack within a segment, (b) Fragment of segment at a longitudinal joint, (c) Fragment of segment at a circumferential joint, (d) Apparent dislocation between segments.

the tunnel is significantly less than the grouting pressure. Thus, the grouting pressure is large enough to compress the soil and change the stress distribution on the tunnel segments, causing segments movement and track bed uplift.

(iii) The volume of secondary grouting depends on the gap between the segment and soil. In general, most of the gaps had been filled by synchronous grouting during the construction of the tunnel. The post-failure investigation indicated that the volume of slurry injected during the secondary grouting (shown in Table 4) was too high, which caused the segments to move. The finding is supported by observations of slurry infiltration inside the tunnel at some segments' joints during the secondary grouting works.

(iv) The injection positions of the secondary grouting were not selected as symmetrical. The resulting asymmetric grouting might have caused uneven stress around the segments and thus uneven movement of the segments and inconsistent breakage on both sides of the tunnel. By comparing the uplift data and grouting positions, it can be found that the uplift of the track at the grouting sides are larger than the other side without grouting.

In summary, the observed damages in the tunnel are most likely due to improper application of the secondary grouting, which is mainly caused by poor selection of the injection pressure, volume and locations. Following this investigation, the next challenge was to assess the state of segments to inform the planning of the repair work.

7. Tunnel inspection using Ground Penetrating Radar (GPR)

Before developing any repair strategy, further inspection of the tunnel was necessary to assess the condition of the segments, the grouting distribution and any void that might had been created by the application of secondary grouting. Ground Penetrating Radar (GPR) was selected to inspect the tunnel as it is a non-destructive surveying method. The concept and advantage of GPR for tunnel investigations are explained elsewhere (e.g. Zhang et al., 2010).

An SIR-3000 GPR, produced by Rauray Ltd with 400 MHz antenna, was used (Fig. 8) to scan both the floor (track bed) and the roof in the following zones: (i) The secondary grouting zones where uplift or uplift slope reached its maximal value, (ii) The transition zones between areas with and without secondary grouting as these zones were the most likely to experience disturbance due to secondary grouting.

The interpretation of GPR results is shown in Fig. 9. The maximal thickness of the track bed is about 80 cm, and the thickness of a segment is 30 cm. The figure also shows the grouting zones around the segments, including previous synchronous grouting and later secondary grouting, with a thickness of 20–40 cm. The fold wave shown in the track bed is the reflected wave of the reinforcing bar. Analysis of the GPR detection signal identified no voids under the track bed or above the roof within the scanned zones.

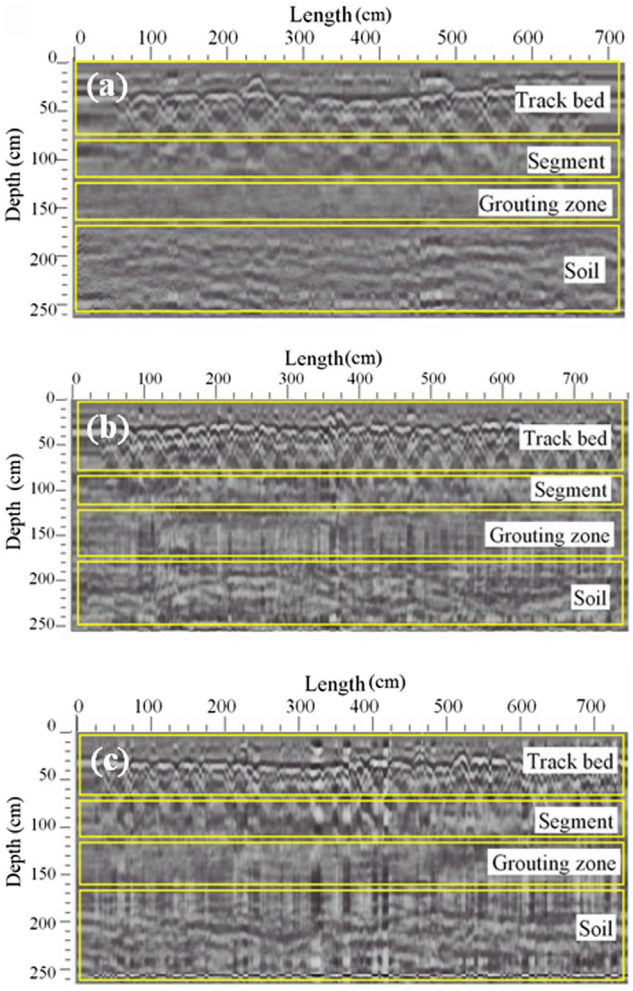

Fig. 9. Interpretation of GPR scanning: (a) Typical section at the maximal uplift are, (b) Typical section at the maximal uplift slope area, (c) Typical section at the area without secondary grouting.

8. Repair strategies

Following the tunnel inspection, the damaged and leaking segments, as well as the track, were repaired using the methods and procedures explained below.

8.1. Repair of cracks

Repair strategies of cracks generated in the segments (see Fig. 7)

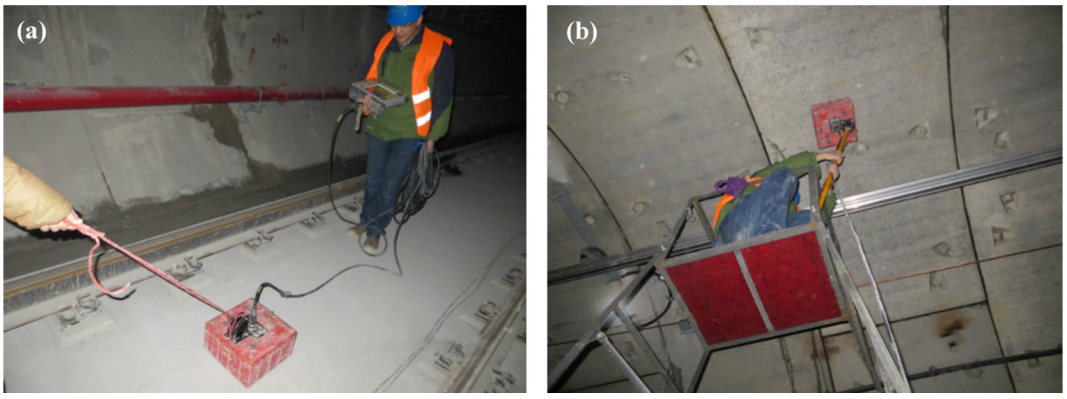

Fig. 8. Photos showing the GPR scanning of the tunnel: (a) Scanning of tunnel floor, (b) Scanning of tunnel roof.

adopted the following criteria:

(1) Defective segments above the centre line of the tunnel were not repaired, based on the experience of high-speed railway tunnels in China. Instead, the rupture surface of segments was cleaned and protected with concrete anticorrosive paint and, if exposed, the reinforcing bars were sprayed with anti-rust paint.
(2) Segments below the centre line of the tunnel, with crack depths greater than 5 cm or crack areas larger than 20 cm^2, were repaired as follow:
   a. The patching materials included ordinary Portland cement of 52.5 grade and ordinary white Portland cement of 42.5 grade, sand with fineness modulus of 2.5–2.8, gravel with a diameter of 5–8 mm, white or colourless liquid concrete patching glue, concrete interface bonding agent and concrete adhesive.
   b. A reinforcement bar (with a planted depth no less than 100 mm and the same specifications as the original bar in the segment) was planted at the crack area before repairing. A hole for reinforcing the bar was installed with an electric drill, and the reinforcing bar was fixed with chemical adhesive. The spacing of this chemical rebar-planting was about 80–100 mm. Transverse reinforcement was added and welded securely with a planting reinforcing bar when the cracked concrete area of the segment was found very big. No expansion bolts were used because these bolts might open up the subsequent repaired concrete and crack it.
   c. The concrete that had broken loose from the segment was removed completely with a steel chisel and hammer, after planting the reinforcing bar. Following the removal, a concrete interface treatment agent with a suitable viscosity was painted on the broken concrete surface. Before the solidification of the interfacial treatment agent, the broken concrete surface was repaired with layers of high strength concrete, each layer with a thickness of no more than 20 mm and a time interval of 5–6 h.
   d. The weight mix proportions used in the high strength concrete were 1.0: 1.5: 1.5: 0.4: 0.3 (ordinary Portland cement: sand: gravel: concrete mending adhesive: water).
(3) Those segments below the centre line of the tunnel, with crack depths of less than 5 cm and crack areas of less than 20 cm^2, were repaired as follows:
   a. Planting a reinforcement bar was not required during the segments' repair, and step (2)-c was followed as explained above.
   b. The weight mix proportions used in the high strength mortar were 1.0: 3.0: 0.4: 0.3 (ordinary Portland cement: sand: concrete mending adhesive: water).
   c. Any material plugging the segments' joints was removed and cleaned before repairing the segments.

8.2. Repair of leakage

The treatment of leaking segments (see Fig. 5) used different strategies depending on the location of the leakage:

(1) Leakage at segments' joints
   Although leakage emerged at segments' joints, the post-failure investigation revealed that the rubber waterstops within them were only partially damaged and capable of providing an adequate water sealing. Therefore, the rubber waterstops were not disturbed any further during the leakage treatment. This was achieved by installing injection needles at the leakage sites and carefully injecting polyurethane material. The method was implemented in five steps:
   a. Removing and cleaning the mud or dirt from the segment joints with a wire brush.
   b. Installing injection needles at leakage sites in the segments' joints, with a depth of 20 cm and a spacing of 30 cm.
   c. Pointing the joints at the leakage sites with quick-setting cement slurry.
   d. Injecting polyurethane into the leakage sites through injection needles with an injection pressure of 1.0–0.2 MPa. If there was still leakage at the joints after two hours of the injection, polyurethane was injected again until seepage stopped.
   e. Removing the injection needles and cleaning any slurry covering the segment surface. A decoration treatment was also conducted at the joints for an improved finish if necessary.
(2) Leakage at grouting holes
   When the amount of leakage at a grouting hole was minimal, the hole was cleaned first and then filled with fast hardening micro expansive cement, and then plugged tightly. If there was still leakage after the treatment, a hole was drilled on the plug, and an injection needle was installed in the drilling hole, and polyurethane was injected through the needle until the leakage stopped. For grouting holes with significant leakage, binary slurry mixed with cement and soluble silicate was injected through the valve installed in the grouting hole.
(3) Leakage at bolt holes
   The leakage at a bolt hole is usually caused by leakage from the neighbouring segment joints thus treatment should also consider the neighbouring joints. Therefore, both ends of any bolt hole identified with leakage problem were filled with fast hardening micro expansive cement firstly, and then polyurethane was injected into the segment joints at the middle of the two corresponding bolt holes. The leakage stopped when the bolt holes were filled with polyurethane.
(4) Leakage at cracked edges of segments

When leakage was located at a cracked edge of a segment, the cracked concrete area was repaired first as described in Section 8.1.

Fig. 10. Photos showing some the works of leakage treatment.

Then the leakage was treated in a similar way as described in Section 8.2(1).

Fig. 10 shows photos taken during the leakage treatment carried out for the tunnel. It was very important during this work to avoid damaging the rubber waterstops in the segments' joints by drilling or other intrusive operations. It was also important to monitor the injected volume of polyurethane and check for any sign of spillage so that appropriate action could be taken. For instance, during the work on one of the treated segments, work had to be stopped after about 5 min of polyurethane injection as the volume of the injected slurry was insignificant but spilled out of the joints. In this situation, the work was not restarted until the situation had been adequately inspected. It was also important to monitor the value of the pressure gauge carefully and ensure it was within the selected range during the polyurethane's injection. All the connections of machine, equipment, pipe and connector were firmly fixed to prevent blasting during operations. In addition, because polyurethane is a solvent and combustible, good ventilation and avoidance of exposure to fire sources during its application were maintained.

8.3. Repair of track and track bed

As mentioned above, different degrees of uplift of track and track bed occurred due to the application of secondary grouting, causing changes in the slope of the track such that it did not meet the design requirements. Repairing of the track in the affected areas was thus required. The elevation of track could be adjusted through changing the thickness of track backing plate within an adjustment range of between 4 and 20 mm. The adjustment approach was adopted for most of the affected areas. However, the uplift of the track reached a maximum value of 88 mm, which is outside the range of adjustment that can be possibly achieved. When the elevation of track goes beyond the possible adjustment range, the original track bed can not be used anymore. For these areas, the track bed was rebuilt to accommodate the required track elevation and to ensure a firm connection between track and track bed.

Following the completion of the repair work, further inspection of the tunnel was carried out for quality assurance. The inspection suggested that the repaired track, segments and leakage met the design requirements. Finally, the repaired section of Hefei metro line 1 was reopened at the end of 2016.

9. Conclusion

This paper presents a case study on the unsuccessful implementation of secondary grouting carried out for a shield tunnel in Hefei city, China, to highlight lessons learned and propose simplified repairing strategies that can be used by tunnel engineers involved with similar maintenance work.

Secondary grouting has been used to treat leakage issues discovered at several locations including segments' joints, bolt holes and grouting holes. However, after one week of starting the secondary grouting, the site survey found that the track and track surface had been uplifted unevenly with maximal uplift of 8.8 cm. Different structural problems in segments associated with differential uplift were observed, such as cracks, fragments and dislocation. The investigation confirmed that the situation had been caused by high grouting pressure and significant volume of slurry injected during the grouting work. In addition, the injection positions of the secondary grouting were asymmetrically selected across the treated tunnel sections. This asymmetrical grouting might have caused uneven stress around the segment and thus inconsistent damage on both sides of the tunnel line.

Although the grouting pressure used in this work was within the range (0.2–0.4 MPa) recommended by tunnelling industry in China, the selected upper-bound value of 0.4 MPa was clearly not appropriate. A careful selection of this pressure is best informed by a reliable assessment of the in-situ stress (geostatic pressure) and the ground conditions surrounding the tunnel.

GPR scanning was a viable non-invasive option for inspecting the condition of the tunnel to detect voids below the track bed (including the grout and soil) to inform the repair strategies. Results from the GPR scanning revealed there were no voids below the track bed within the affected zones of the tunnel.

Simplified strategies were presented in this study for repairing the tunnel's defects including segments' cracks, leakage and uplifted track. The adopted strategies were successfully able to avoid any further damage to the segments and to restore the affected section of the tunnel to the required conditions.

The findings of this case study strongly suggest that secondary grouting may be better implemented before the construction of the track and track bed, particularly if there is uncertainty in the design of the secondary grouting, particularly the selection of injection pressure in relation to in-situ geostatic pressure. By adopting this approach, the potential damage to the track and track bed of the tunnel can be avoided.

Acknowledgements

This work was financially supported by Anhui Provincial Department of Education program for visiting professors (grant No. gxfxZD2016216) and Hefei University academic leaders' project (grant No. 2016dtr01). The authors express their appreciation to the project department of China railway 24th Bureau Group Co., Ltd. for providing survey data and documentation of this case study.

References

Butrón, C., Gustafson, G., Fransson, Å., Funehag, J., 2010. Drip sealing of tunnels in hard rock: a new concept for the design and evaluation of permeation grouting. Tunn. Undergr. Space Technol. 25, 114–121.

Chi, J.P., 2015. Experimental study on control of water leakage of primary support of tunnel of Qingdao metro by micro-cement grouting. Tunnel Constr. 35 (8), 759–765 (in Chinese).

Gou, C.F., 2013. Study on the Grouts Diffusion Mechanism of Shield Tunnel Back-filled Grouts. Chang'an University, Xi'an (in Chinese).

Guo, S.Y., Wan, J.L., 2004. Design and development of monitoring systems for road tunnels. Mod. Tunn. Technol. 41 (4), 1–6 (in Chinese).

He, C., Feng, K., Fand, Y., 2015. Review and prospects on constructing technologies of metro tunnels using shield tunnelling method. J. Southwest Jiaotong Univ. 50 (1), 97–109 (in Chinese).

Komiya, K., Soga, K., Akagi, H., Jafari, M.R., Bolton, M.D., 2001. Soil consolidation associated with grouting during shield tunnelling in soft clayey ground. Geotechnique 51 (10), 835–846.

Kasper, T., Meschke, G., 2006a. A numerical study of the effect of soil and grout material properties and cover depth in shield tunnelling. Comput Geotech 33, 234–247.

Kasper, T., Meschke, G., 2006b. On the influence of face pressure, grouting pressure and TBM design in soft ground tunnelling. Tunn. Undergr. Space Technol. 21, 160–171.

Li, H.Y., 2014. Study on Deformation Mechanics and Support Mechanical Behaviour of Large-span Shallow-buried Tunnel in Expansive Ground. Southwest Jiaotong University, Chengdu Doctoral dissertation (in Chinese).

Li, S.C., Liu, R.T., Zhang, Q.S., Zhang, X., 2016. Protection against water or mud inrush in tunnels by grouting: a review. J. Rock Mech. Geotech. Eng. 8 (5), 753–766.

Li, W., He, C., Xie, H.Q., 2006. Study on the control pressure of secondary grouting for shield tunnel in rock under high water pressure. China Rail. Sci. 27 (1), 32–37 (in Chinese).

Ministry of Construction of the PRC, 1999. Code for Construction and Acceptance of Metro Engineering (GB50299-1999). China Planning Press, Beijing (in Chinese).

Ministry of Construction of the PRC, 2008. Technical Code for Waterproofing of Underground Works (GB50108-2008). China Planning Press, Beijing (in Chinese).

Stille, B., Gustafson, G., 2010. A review of the Namntall Tunnel project with regard to grouting performance. Tunn. Undergr. Space Technol. 25, 346–356.

Tang, J.J., Huang, J., Zhou, Y.X., Wang, P.R., 2016. Study progress of synchronous grouting material for shield tunneling method. Modern Urban Transit 4, 89–92 (in Chinese).

Wu, H.N., Shen, S.L., Ma, Y.H., Liu, Y.B., Du, S.J., 2013. Investigation and analysis on the leakage of the river-crossing tunnels in Shanghai. Chinese J. Undergr. Space Eng. 9 (3), 663–668 (in Chinese).

Ye, F., 2007. Analysis and Control for Upward Movement of Shield Tunnel During Construction. Tongji University, Shanghai (in Chinese).

Ye, F., Mao, J.H., Ji, M., Sun, C.H., Chen, Z., 2015. Research status and development trend of back-filled grouting of shield tunnels. Tunn. Constr. 35 (8), 739–752 (in Chinese).

Yong, B.Y., Breitenbücher, R., 2014. Influencing parameters of the grout mix on the properties of annular gap grouts in mechanized tunnelling. Tunn. Undergr. Space Technol. 43, 290–299.

Zhang, F.S., Xie, X.Y., Huang, H.W., 2010. Application of ground penetrating radar in grouting evaluation for shield tunnel construction. Tunn. Undergr. Space Technol. 25, 99–107.

Zheng, P.Y., 2015. Analysis of secondary grouting technology in shield tunnel of water-rich gravel stratum. Constr Archit. 12, 68–70 (in Chinese).